

## Chapter 2

### Description of the Pair Weight Method with no Redshift Distortions

The prospect of large, well-controlled redshift surveys such as the Two-Degree Field Survey (2dF) and the Sloan Digital Sky Survey (SDSS) and their potential for constraining cosmological parameters (Peacock 1997; Eisenstein et al. 1999) has motivated an increasing level of sophistication in the measurement of galaxy power spectra.

In recent years two approaches to measuring power spectra from galaxy surveys have come to the fore (Tegmark et al., 1998). The first is the ‘brute-force’ method, the linear maximum likelihood method pioneered by Fisher et al. (1994) and Heavens and Taylor (1995). The second is the ‘classical’ method (Feldman et al., 1994, hereafter FKP; Hamilton 2000). The two methods are complementary to each other, each performing best where the other method does the worst: the brute-force method works best at large scales, while the classical method works best at smaller scales.

Both brute-force and classical methods lay claim to being ‘optimal’ provided that certain assumptions are true. The defining assumption of the brute-force method is that density fluctuations are Gaussian. Thus the brute-force method is the method of choice at the largest, linear scales, where fluctuations may well be Gaussian. The brute force method has been applied to the *IRAS* 1.2 Jy survey by Heavens and Taylor (1995) and Ballinger et al. (1995), to the *IRAS* Point Source Catalogue redshift (PSCz) survey by Tadros et al. (1999), and to the Updated Zwicky Catalog (UZC) by Padmanabhan et al. (2000).

The defining assumption of the classical method is that the selection function  $\bar{n}(\mathbf{r})$  of a

survey, the probability of selecting a galaxy at position  $\mathbf{r}$  into the survey, is ‘slowly varying’. The classical method is good to the extent that position and wavelength of the fluctuation can be measured simultaneously. In quantum mechanics, this is the condition for a system to be classical – hence the designation. The classical method is optimal for measuring power at wavelengths much less than any characteristic scale of the survey, such as the scale over which the selection function varies.

The classical method was introduced by Feldman et al. (1994) for the case of Gaussian fluctuations. However, the method can be generalized into the nonlinear regime (Hamilton 2000). In this chapter the expression ‘classical’ refers, in general, to the nonlinear generalization of the FKP method.

While the brute-force method should be optimal at the largest scales of a survey, and the classical method should be optimal at the smallest scales, it can happen that both methods are suboptimal at intermediate scales. In the Las Campanas Redshift Survey (LCRS), for example, the width of each of the six  $1.5^\circ$  slices is  $\sim 7.5 h^{-1} \text{Mpc}$  at the median depth  $\sim 300 h^{-1} \text{Mpc}$  of the survey. Density fluctuations at this wavelength are neither fully linear nor much smaller than the scale of the survey.

The brute-force and classical estimators of the power spectrum remain unbiased (or at least asymptotically unbiased) even where they are suboptimal (Tegmark et al., 1997; Hamilton 2000). In other words, the estimators are valid estimators of the power spectrum, being biased neither high nor low, even if they are not the best estimators. However, both methods yield incorrect error bars on the power spectrum in regimes where their assumptions fail. For example, at nonlinear scales the brute-force method grossly underestimates the variance in the estimated power spectrum, by a factor  $\sim 1 + \xi$  where  $\xi$  is the correlation function. Thus, in general, it is necessary to resort to some additional procedure to compute reliable error bars. For example, error bars can be estimated from ensembles of  $N$ -body simulations (*e.g.*, Fisher et al., 1993), or empirically from the level of fluctuations observed in the data (Maddox et al., 1990; Hamilton, 1993).

The purpose of the present chapter is to explore a new method for constructing a near-optimal estimator of the power spectrum. The method goes beyond the classical approximation, but is not restricted to linear, Gaussian fluctuations. Among other things, the method is designed to yield correct error bars on the power spectrum.

Recall that in the original linear FKP approximation, the power spectrum  $P_k$  at wavenumber  $k$  is measured by weighting overdensities in pairs  $ij$  of volume elements at positions  $\mathbf{r}_i$  and  $\mathbf{r}_j$  with a pair weighting of the form

$$W_{ij} = \frac{\bar{n}_i \bar{n}_j}{(1 + \bar{n}_i P_k)(1 + \bar{n}_j P_k)} \quad (2.1)$$

where  $\bar{n}_i \equiv \bar{n}(\mathbf{r}_i)$  is the selection function at position  $\mathbf{r}_i$ . The idea of the present chapter is to admit not just a single pair weighting, as in the classical FKP method, but rather several pair weightings, judiciously chosen. In effect, the power spectrum is ‘compressed’ (Tegmark et al., 1997) into several measurements of it using different pair weightings; the several measurements of the power spectrum are then combined using their Fisher matrix. The procedure is at least somewhat familiar. For example, Fisher et al. (1993), FKP, and Sutherland et al. (1999) present measurements of the power spectrum using not one but several different pair weightings. (In the last two papers, the pair-weightings were linear FKP pair-weightings of the form of equation [2.1], with the quantity  $P_k$  in the denominator treated as an adjustable constant). The present method goes a step further by combining estimates from different pair-weightings, using their Fisher matrix.

Using the Fisher matrix to merge estimates of the power spectrum takes into account the covariance between the estimates and automatically yields the best possible combination of the estimates. In principle, an optimal measurement of the power spectrum could be obtained in the limit of many estimates of power spectra derived from a large number of different pair weightings. In practice, numerics limit the number of pair weightings that can be handled to only a few. Still, even just two sets of pair weightings is better than a single pair weighting.

For simplicity, and to facilitate comparison with other methods, the present chapter is

limited to the case of Gaussian fluctuations without redshift distortions. We include redshift distortions in later chapters and hope to include non-linearity in future work.

There is a parallel between the approach proposed in the pair weight method and the linear brute-force method for Gaussian fluctuations. In the linear brute-force method, the data in a galaxy survey, the overdensities  $\delta_i$  in many volume elements  $i$ , are compressed into a set of linearly weighted modes  $\hat{x}_a \equiv W_{ai}\delta_i$ . To retain as much information as possible, the number of modes should be as large as possible; but numerical tractability limits the number of modes to several  $\times 10^3$  or possibly several  $\times 10^4$ . The game is then to craft the modes so as to cram the largest amount of information about parameters of interest (*e.g.*, the amplitude  $P_k$  of the power spectrum at several linear wavenumbers  $k$ , and the redshift distortion parameter  $\beta \approx \Omega^{0.6}/b$ ) into the smallest number of modes (Heavens and Taylor 1995; Tegmark et al. 1997; Padmanabhan et al. 2000). Here, the data are compressed, instead, into a set of quadratically weighted modes  $\hat{X}_a = W_{aij}\delta_i\delta_j$ . The game is similar: try to choose the pair windows  $W_{aij}$  so as to cram the largest amount of information into the smallest number of pair modes.

One advantage of a quadratic weighting method is that, unlike the linear brute-force method, it is not limited to Gaussian fluctuations. Thus if a nonlinear prior is used (which, however, is not done in this work), then the quadratic weighting method will yield reliable error bars on the nonlinear power spectrum; whereas the linear weighting method will underestimate the true error bars in the nonlinear regime. A disadvantage of the quadratic weighting method is that it is numerically much more involved to compute the Fisher matrix of a set of pair weighted modes, so that in practice only a handful of pair modes can be computed. The situation is not hopeless, however, because a single pair weighting – the linear FKP pair weighting, equation (2.1) – probably already contains a large fraction of the information of interest (Heavens et al., 2000). Adding just one additional pair window is guaranteed to increase the information content of the estimate and to reduce the error bars correspondingly. The gain should be greater in surveys with more complicated selection functions, such as the LCRS.

We describe the pair weight compression method in section 2.1. In section 2.2 we de-

scribe how we actually go about calculating the matrices necessary to obtain the measurements. Section 2.3 compares the Fisher matrices for IRAS 1.2 Jy and LCRS using the classical method and the pair weight compression method. In section 2.4 we discuss the method, our results, and possible applications.

## 2.1 Pair Weight Compression

We introduce here, in subsection 2.1.2, the pair weight compression scheme for measuring the power spectrum from a galaxy survey. We begin by reviewing, in subsection 2.1.1, the linear compression scheme (Tegmark et al., 1997), which is the basis of the standard ‘brute-force’ procedure.

### 2.1.1 Linear Weights

The data contained in a galaxy survey are the values  $n_i$  of the galaxy number density in each of the infinitely many infinitesimal volume elements  $dV_i$  of the survey. To the extent that the selection function  $\bar{n}_i$  is known or can be measured with negligible uncertainty (Binggeli et al., 1988; Willmer, 1997; Tresse, 1999), the data can be taken to be the overdensities  $\delta_i \equiv (n_i - \bar{n}_i)/\bar{n}_i$ .

Suppose that these overdensities are compressed into a set of mode amplitudes  $\hat{x}_a$  (the hat signifies an estimated quantity, distinguishing it from a prior quantity) by weighting the overdensities with a linear weighting function  $W_{ai}$

$$\hat{x}_a \equiv W_{ai}\delta_i \tag{2.2}$$

(repeated Latin indices in eq. [2.2] and hereafter signify implicit integration over the volume element, so  $W_{ai}\delta_i = \int W_a(\mathbf{r})\delta(\mathbf{r})dV$ ; see section 2 of Hamilton, 2000 for an exposition). The covariance of the modes is

$$C_{ab} \equiv \langle \hat{x}_a \hat{x}_b \rangle = W_{ai} \langle \delta_i \delta_j \rangle W_{bj} \tag{2.3}$$

where  $\delta_i \delta_j$  is the expected covariance function of the survey, which is a sum of a signal term, the cosmic correlation function  $\xi(r_{ij})$ , and a noise term, commonly taken to be dominated by Poisson sampling noise

$$\langle \delta_i \delta_j \rangle = \xi_\alpha B_{\alpha ij} + \bar{n}^{-1}(\mathbf{r}_i) \delta_{ij} \quad (2.4)$$

the correlation function with respect to the linear combination of individual parameters  $\xi_\alpha$ .

Any linear combination of Gaussian fields is Gaussian, so if the overdensity field  $\delta_i$  is Gaussian – the defining assumption of the linear method – then the mode amplitudes,  $\hat{x}_a$  will also form a multivariate Gaussian. Gaussian fields have the advantage that the likelihood function can be written down explicitly:

$$\mathcal{L} = \frac{1}{|C|^{1/2}} \exp \left[ -\frac{1}{2} \hat{x}_a C_{ab}^{-1} \hat{x}_b \right]. \quad (2.5)$$

The maximum likelihood estimate  $\hat{\xi}$  of the parameters is given by the vanishing of the derivative of  $\ln \mathcal{L}$  with respect to the parameters:

$$\frac{\partial(\ln \mathcal{L})}{\partial \xi_\alpha} = \frac{1}{2} [C_{ab}^{-1} C_{bc, \alpha} C_{cd}^{-1} (\hat{x}_d \hat{x}_a - C_{da})] \quad (2.6)$$

$$\left. \frac{\partial(\ln \mathcal{L})}{\partial \xi_\alpha} \right|_{\xi=\hat{\xi}} = 0. \quad (2.7)$$

If the parameters  $\xi_a$  are the values of power spectrum at many different wavenumbers  $k_a$ , then the covariance  $C_{ab}$  depends linearly on the parameters

$$C_{ab} = \frac{\partial C_{ab}}{\partial \xi_\alpha} \xi_\alpha + N_{ab}. \quad (2.8)$$

The maximum likelihood estimator  $\hat{\xi}_\alpha$  of the power spectrum is then

$$\hat{\xi}_\alpha = F_{\alpha\beta}^{-1} C_{ab}^{-1} C_{bc, \beta} C_{cd}^{-1} \hat{x}_a \hat{x}_d \quad (2.9)$$

where  $F_{\alpha\beta}$  is the Fisher matrix of the parameters  $\xi_\alpha$

$$F_{\alpha\beta} \equiv C_{ab}^{-1} C_{bc, \alpha} C_{cd}^{-1} C_{da, \beta}. \quad (2.10)$$

Equations (2.9) and (2.10) provide the best (maximum likelihood) estimate of the power spectrum  $\xi_\alpha$  that can be deduced from the given set of modes:  $a$ . If the modes formed a complete set (which would require infinitely many modes), then the estimator would be optimal. However, computational tractability limits the number of modes that can be treated to several  $\times 10^3$  or possibly several  $\times 10^4$ . Thus, a key part of the brute-force method is to try to choose the modes to contain as much information as possible about the parameters of interest, the values of the power spectrum at large, linear scales. This can be achieved by crafting the modes wisely (Heavens and Taylor, 1995) and perhaps also by performing some kind of Karhunen-Loève (signal-to-noise) compression (Vogeley and Szalay, 1996; Tegmark et al., 1997; Tegmark et al., 1998; Padmanabhan et al., 2000).

### 2.1.2 Pair Weight Method

In the pair weight scheme, the overdensities are compressed instead into a set of pair-weighted modes

$$\hat{X}_a \equiv W_{aij} \delta_i \delta_j. \quad (2.11)$$

This seems like a natural thing to do since, after all, the power spectrum is itself an expectation value of a covariance of overdensities. Indeed, the traditional way to measure the power spectrum is based on equation (2.11) with just a single pair weighting  $W_{aij}$ , suitably normalized (that is, one estimates  $\hat{\xi}_\alpha = W_{\alpha ij} \delta_i \delta_j$ , the shot noise being removed by excluding the contribution of self-pairs of galaxies to the estimator). Commonly, some variant of the linear FKP pair-weighting, equation (2.1) is adopted.

The expectation value of the amplitude  $\hat{X}_a$  of the pair mode is

$$\langle \hat{X}_a \rangle \equiv X_a = W_{aij} C_{ij} = W_{aij} B_{\alpha ij} \xi_\alpha + W_{aij} \delta_B(r_{ij}) \bar{n}^{-1}(\mathbf{r}_i). \quad (2.12)$$

The covariance is

$$\langle \Delta \hat{X}_a \Delta \hat{X}_b \rangle = W_{aij} \langle \Delta C_{ij} \Delta C_{kl} \rangle W_{bkl} \equiv W_{aij} \langle \mathbf{c}_{ijkl} \rangle W_{bkl} \equiv K_{ab}. \quad (2.13)$$

In a sufficiently large survey, the central limit theorem implies that the estimator  $\hat{X}_a$  will be Gaussianly distributed about its expectation value. This is true irrespective of whether the underlying density field is Gaussian or not. In practice, surveys typically do contain enough information that  $\hat{X}_a$  will be near Gaussian at all but the largest scales, where the linear brute-force method is the method of choice. We assume therefore that  $\hat{X}_a$  are Gaussianly distributed, so that the likelihood function is

$$\mathcal{L} \propto \frac{1}{|K|^{1/2}} \exp \left[ -\frac{1}{2} (\hat{X}_a - W_{aij} B_{\alpha ij} \xi_\alpha) K_{ab}^{-1} (\hat{X}_b - W_{bkl} B_{\beta kl} \xi_\beta) \right]. \quad (2.14)$$

Take the derivative of  $-\ln \mathcal{L}$  with respect to  $\xi_\alpha$  and set the result to zero to find the estimate of  $\xi_\alpha$  given the set of pair weights in the model.

$$\begin{aligned} \frac{\partial(-\ln \mathcal{L})}{\partial \xi_\alpha} &= \frac{1}{2} K_{dc}^{-1} K_{dc, \alpha} - \\ &\frac{1}{2} (\hat{X}_a - \xi_\alpha B_{\alpha ij} W_{ija}) K_{ac}^{-1} K_{cd, \alpha} K_{db}^{-1} (\hat{X}_b - W_{bkl} \xi_\beta B_{\beta kl}) - \\ &W_{aij} B_{\alpha ij} K_{ab}^{-1} (\hat{X}_b - W_{bkl} \xi_\beta B_{\beta kl}) B_{\beta kl}. \end{aligned} \quad (2.15)$$

Take the first two terms and rewrite them as

$$\frac{1}{2} K_{ac}^{-1} K_{cd, \alpha} K_{db}^{-1} [K_{ba} - (\hat{X}_b - W_{bkl} \xi_\beta B_{\beta kl}) (\hat{X}_a - \xi_\alpha B_{\alpha ij} W_{ija})]. \quad (2.16)$$

In order to perform the full maximum likelihood calculation these terms must be calculated explicitly. Bond et al. (1998) show that it is possible to carefully include the contribution from these terms. However, Tegmark et al. (1997) shows that the estimator is asymptotically unbiased even if it is suboptimal. In the minimum variance case, the derivatives of  $K$  are set to zero and these terms vanish. In the remainder of this thesis, we take the minimum variance solution rather than the full maximum likelihood solution. This leaves:

$$-W_{aij} B_{\alpha ij} K_{ab}^{-1} (\hat{X}_b - W_{bkl} \hat{\xi}_\beta B_{\beta kl}) = 0. \quad (2.17)$$

Rearrange this equation and replace  $\hat{X}_b$  with  $W_{bkl} \delta_k \delta_l$  to get:

$$B_{\alpha ij} W_{aij} K_{ab}^{-1} W_{bkl} B_{\beta kl} \hat{\xi}_\beta = B_{\alpha ij} W_{aij} K_{ab}^{-1} W_{bkl} \delta_k \delta_l. \quad (2.18)$$

Define a new matrix (the Fisher matrix)  $M$ :

$$M_{\alpha\beta} \equiv B_{\alpha ij} W_{aij} K_{ab}^{-1} W_{bkl} B_{\beta kl}. \quad (2.19)$$

In order to get the final estimate of  $\xi_\alpha$ , multiply both sides of equation (2.18) by the inverse of  $M$ . The final result is

$$\hat{\xi}_\beta = M_{\beta\alpha}^{-1} B_{\alpha ij} W_{aij} K_{ab}^{-1} W_{bkl} \delta_k \delta_l. \quad (2.20)$$

This gives us a complete method for calculating  $\hat{\xi}_\alpha$  using the multiple pair weights  $W_{aij}$ . We can see that we no longer have to invert the  $C$  matrix directly. On the other hand, we must make sure that the computation of the matrix  $K$  is feasible. If we assume Gaussian fluctuations then

$$\langle \mathfrak{C}_{ijkl} \rangle \approx C_{ik} C_{jl} + C_{il} C_{jk}. \quad (2.21)$$

The matrix  $K$ , Equation 2.13, can then be rewritten as:

$$K_{ab} \approx 2W_{aij} C_{ik} C_{jl} W_{bkl}. \quad (2.22)$$

It is not necessary to make this particular approximation. However, we do need a prior estimate for  $\langle \mathfrak{C}_{ijkl} \rangle$ .

In principle, the pair weighting method can save computation time over a brute force technique, particularly for size scales significantly smaller than the size of the catalog. For example, doubling the resolution in the pair weight method takes four times as much computing capacity, instead of the  $\sim 2^9$  (based on the computing cost of matrix inversion which is an  $n^3$  process) times for a brute force method. (The computation of  $K$  is the slowest part, and on average each matrix element takes the same amount of time. Doubling the resolution requires four times as many matrix elements.) The down sides are that the creation of the matrix  $K$  loses information if the choice of pair weights is not complete, and the matrix  $K$  can also be quite computationally expensive. The matrix  $M$  can be used as the Fisher information matrix.

$$M_{\alpha\beta} \equiv B_{\alpha ij} W_{aij} K_{ab}^{-1} W_{bkl} B_{\beta kl} = B_{\alpha ij} W_{aij} W_{amn}^{-1} F_{mnop} W_{bop}^{-1} W_{bkl} B_{\beta kl} \quad (2.23)$$

where  $F_{mnop}$  is the Fisher matrix with respect to parameters  $\sum_{\alpha} \xi_{\alpha} B_{\alpha mn}$  and  $\sum_{\beta} \xi_{\beta} B_{\beta op}$ . To the extent that the choice of windows is a complete set

$$W_{aij} W_{amn}^{-1} \approx \delta_{im} \delta_{jn}. \quad (2.24)$$

This means that by applying the chain rule and noting that  $\frac{\partial C_{ij}}{\partial \xi_{\alpha}} = B_{\alpha ij}$

$$M_{\alpha\beta} \approx B_{\alpha ij} F_{ijkl} B_{\beta kl} = F_{\alpha\beta}. \quad (2.25)$$

This means that we can compare the pair weight method to another method by comparing the resulting Fisher matrices. In the case of the pair weight method we will insert  $M$  in place of  $F$ . If  $M$  is identical to the Fisher matrix as computed by an exact method then we know that the pair weight method loses no information. We will see in the next section that the difficulty in the pair weight method lies in the computation of  $K$ .

## 2.2 Calculation of the Pair Weight Fisher Matrix

Equation (2.25) says that the matrix  $M$  is equivalent to the Fisher matrix. Calculating  $M$  requires the matrices  $K_{ab}$  and  $B_{\alpha ij} W_{aij}$ . This section discusses the method of calculation for  $K_{ab}$  since it is by far the more difficult of the two. The calculation of  $K$  requires a 10-dimensional integral (equation 2.22), to be performed. (Each of the four volume elements contributes 3 dimensions and each window function  $W_{aij}$  and  $W_{bkl}$  involves a delta function which effectively removes a dimension.) for each pair of values  $a$  and  $b$ . There are two serious complications: the volume elements are linked by the correlation function of the separation of two pairs of two elements (this makes it impossible to reduce the 10-dimensional integral to a product of smaller integrals) and the lack of full-sky coverage. (This removes possible symmetries making analytical progress difficult). We therefore proceed by Monte Carlo techniques.

### 2.2.1 Nonuniform Monte Carlo Integration of $K$

Monte Carlo integration is a technique by which one integrates by randomly selecting points within the range of integration and computing the average value of the integrand (as

well as the average of the integrand squared) over those points. For a good introduction to the subject, see *Numerical Recipes* (Press et al., 1986). Monte Carlo integration relies on the idea that

$$\int \rho dr = \bar{\rho} \int dr \quad (2.26)$$

for the average  $\bar{\rho}$ . We can then approximate

$$\bar{\rho} \approx \frac{1}{n} \sum_{i=1}^n \rho(r_i) \quad (2.27)$$

where the values  $r_i$  are randomly chosen to be within the range of the integral. The accuracy to which the integral can be calculated depends on how well the average of the points selected represents the true average. Use the average of the integrand squared to estimate the accuracy of the calculation:

$$\Delta \bar{\rho} \approx \left[ \frac{\frac{1}{n} \sum_n \rho^2(r_i) - \bar{\rho}^2}{n} \right]^{\frac{1}{2}}. \quad (2.28)$$

There are two ways to improve the accuracy of the Monte Carlo integration. First, choose more points (increase  $n$ ). As the number of points increases, the average tends towards the true average. Second, we would like  $\rho$  to be as close to constant as possible within the range of integration (so that  $\rho^2$  is very nearly  $\bar{\rho}^2$  for all points) thereby decreasing the numerator in equation (2.28). To do this, change the variable of integration to smooth out  $\rho$ . For example, suppose that  $\rho = r^2(1 + \epsilon(r))$ , where  $|\epsilon| \lesssim 1$ , and the integral runs from  $r = 0$  to  $r = 2$ . Change the integration variable from  $r$  to  $u$  where  $u = r^3$ .

$$\int_0^2 \rho(r) dr = \frac{1}{3} \int_0^8 (1 + \epsilon(u^{\frac{1}{3}})) du. \quad (2.29)$$

By changing the variable from  $r$  to  $u$ , the integrand becomes very nearly constant. This is the equivalent to putting many points in the regions where the integrand is highest and down-weighting the contribution from each of the points in this region. In order to maintain the accuracy of the integral, lower the probability of choosing a point in a low density region and

correspondingly raise the weight given to that point. By smoothing out the contributions from each point, the integral can be calculated to the same accuracy with fewer points.

$K_{ab}$  is a whole matrix of integrals ( $a$  and  $b$  are matrix indices), so they need to be calculated quickly. To this end, choose integration variables to smooth out the entire integral. Fortunately, for the integral  $K$ , this is possible. Equation (2.28) says that the values of  $\rho$  that increase  $\Delta\bar{\rho}$  the most are the largest absolute values. Even though the integral is quite complicated, it is not hard to see which configurations of the four volume elements contribute the most to the integral. First of all, the correlation function is largest when the two volume elements are close to one another, so choose the volume elements in such a way that close pairs (within the volume foursomes) are more likely than more distant pairs. Secondly, the selection function and the chosen window functions vary with distance to the observer. Choosing the volume elements according to the window functions smoothes out the integrand. When the integrand is near zero or exactly zero (outside of the catalog), it contributes relatively little to the error. This only slows down the integral if a high fraction of foursomes has an element outside of the catalog.

### 2.2.2 Step-by-Step Process of Selecting a Galaxy Foursome

To see how the Monte Carlo integration works, it makes sense to look at the process of selecting one galaxy foursome. Equation 2.22 shows the integral that is being performed by Monte Carlo techniques. Each of the indices which is summed over can be thought of as the location of a galaxy. Because there are four summation indices, each location (in twelve-dimensional space with two separations fixed) can be thought of as a galaxy foursome. Figure 2.1 shows one such galaxy foursome for the case of IRAS.

The biggest goal in selecting one of the random variables is to make sure that the selection takes into account everything known about the integral up to that point. This allows the most effective reduction of the largest peaks. Obviously, the first step is to choose the first galaxy. At this point, use the angular mask to make sure that the galaxy will be within the catalog or at least has a good chance of being within the catalog. For a catalog like IRAS 1.2-Jy,

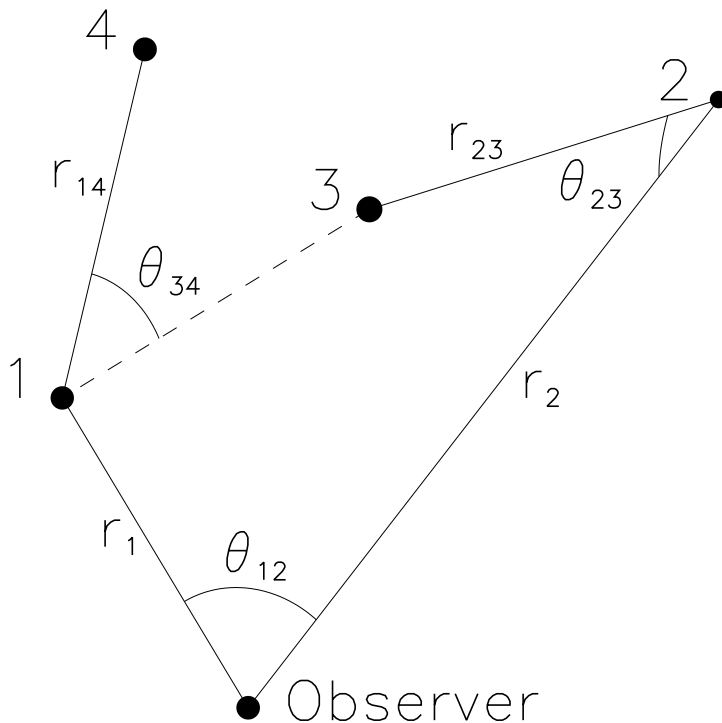


Figure 2.1: A stick figure representation of a galaxy foursome for IRAS.

the angular mask is not a significant issue since more than 90 percent of the sky is within the catalog.

On the other hand, for a catalog like LCRS (less than one steradian of sky coverage), choosing the angular position carefully greatly speeds up the calculation. In LCRS, choose the angular position to lie in one of the six slices in such a way that equal angular areas get equal weight. Figure (2.2) shows the LCRS angular mask. Each square represents one observing area. The fraction of galaxies for which redshifts were obtained is shown by the darkness of the square. (If all galaxies have redshifts then the square is black.) Cross-hatched areas are from

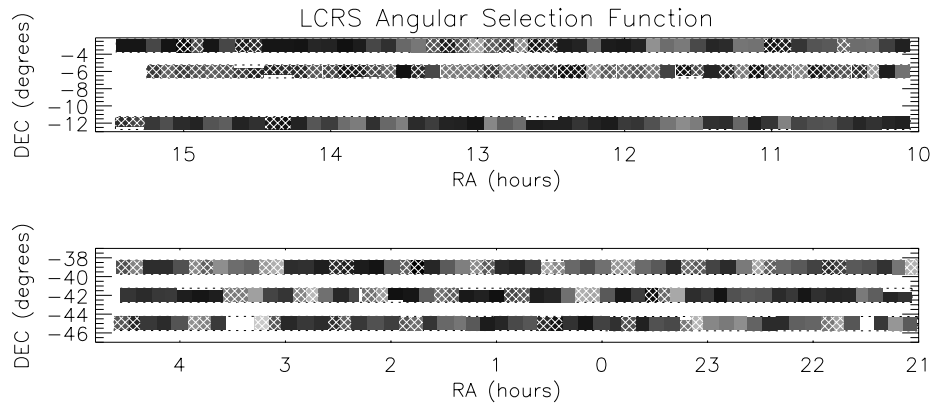


Figure 2.2: The angular selection function for LCRS. The grayscale shows the fraction of galaxies within the region for which redshifts are included. (Black is 100 per cent and white is zero.) Areas which are cross-hatched are from the 50-fiber instrument whereas solid regions are from the 112-fiber instrument.

the first stage of the catalog where 50 redshifts could be obtained simultaneously. Solid squares are from the second stage where 112 redshifts could be taken simultaneously. The dashed lines represent the outer boundaries of the slices. If the galaxy is within one of the slices, it has a very high probability (again over 90 percent) of being in the catalog. Because the slices are not complete, make sure the actual angular position is, in fact, within the catalog. If it is not, then give this galaxy foursome zero weight and move on to the next galaxy foursome. Now go about choosing the radial position of the first galaxy. Make sure that the radial position reflects the chosen window for the matrix element in question. To do this, fit the window function (times the volume at that radius) with a series of power laws. This allows rapid computation of the randomly selected radial position, while at the same time smoothing out the radial peaks. In fact, the distribution of probabilities and the corresponding weights for the radial position of the first galaxy can be precomputed.

In selecting the second galaxy, take into account not only the information about the catalog as a whole but also the position of the first galaxy. The information about the first galaxy is important because one product of the integrand is the correlation function at the separation between galaxies one and two. This means that the integrand is, in general, higher if galaxies

one and two are close together. To eliminate the peaks, increase the probability that these two galaxies are close together and decrease the probability that they are far apart. First select the radial component of the galaxy. Rather than just using the power law fits to the window function, modify the power laws such that the region near the radial component of the first galaxy is more likely to be selected for the second galaxy as well. In other words, increase the power of the power laws for regions smaller than  $r_1$  and decrease the power of the power laws for regions greater than  $r_1$ .

After choosing the radial position, the strategy for choosing the angular position is different for IRAS than it is for LCRS due to the nature of their angular masks. In the case of IRAS, calculate the correlation function for a series of points for given test angles ( $\theta_{12}$ ) between galaxy one and galaxy two. Then fit a series of power laws to the absolute values of the correlation function. (Don't allow any of these points to drop below a lower boundary for two reasons. First, the correlation function can go through zero and negative values can cause problems. Second, giving one section too little probability can cause a new peak to form when a point within this improbable region is chosen due to its large up-weighting.) Then choose the angle between galaxies one and two using these power laws as the probability. The azimuthal angle is chosen with all angles receiving equal probability.

For LCRS, choose the slice and then the location within that slice. Choose the slice with the probabilities given by the angular area of the slice times the maximum of the correlation function with the galaxy in that slice. Choose the latitude within that slice uniformly. (The slices are only  $1.5^\circ$  thick so there is not too much variation over the slice.) The longitudinal angle is found by evaluating the correlation function as if the galaxy were at a few locations along the slice. Then, apportion the probability to locations according to the corresponding values of the correlation function. Again, check that the particular angular position of the galaxy is within the valid portion of the catalog.

The third and fourth galaxies are connected to the first two galaxies by the fixed lengths  $r_{23}$  and  $r_{14}$ . Therefore, only two angles are necessary to define the location of each of these

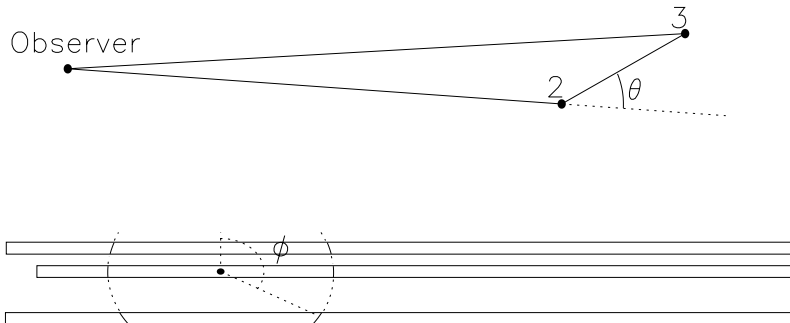


Figure 2.3: Top: definition of  $\theta$  for LCRS. Bottom: depiction of possible choices of  $\phi$  for a given value of  $\theta$ .

galaxies. Define these two angles as  $\theta_{23}$  and  $\phi_{23}$ .  $\theta_{23}$  is the latitudinal angle with its north pole pointing directly toward the center from galaxy two. For IRAS, the contribution to the integral is normally highest if  $\theta_{23}$  is low. This is because the selection function is highest closest to the center. Calculate the selection function for various values of  $\theta_{23}$  and weight the probabilities by these values. Then choose  $\phi_{23}$  with uniform probability.

The situation for LCRS is substantially different. Due to the observing strategy, the selection function is not guaranteed to be larger closer to the center. Therefore, select  $\theta_{23}$  uniformly. Figure (2.3) shows a particular value for  $\theta_{23}$  in the top panel. Use the positions of the slices to guarantee that the value of  $\phi_{23}$  will place the galaxy within one of the slices in the survey (as shown in the bottom panel of Figure 2.3). Once the angular position of galaxy three is known, check to see that it is within the survey. If it is not, (or if no value of  $\phi_{23}$  is within the survey), give this galaxy foursome zero weight and move on to the next foursome.

In the case of the IRAS survey, there are two competing goals in choosing the location of the final galaxy. Positions close to the observer have large selection functions, while at the same time, positions close to galaxy three maximize the correlation function. For simplicity, choose to do one or the other based on the relative importance of the two. If the closest possible separation for galaxies three and four is less than twenty times (empirically the best trade-off)

the smallest possible distance to galaxy four (from the observer), then try to get galaxy four close to galaxy three, as shown in Figure (2.1). Otherwise, try to get it close to the observer. In either case, set up the coordinates such that  $\theta_{34}$  is zero when it minimizes the relevant distance. Then, follow the same procedure for choosing  $\theta_{34}$  as for  $\theta_{23}$ . Once again  $\phi_{34}$  is chosen uniformly.

For LCRS, the selection function is not always decreasing with radius. Therefore, always try to get galaxies three and four close together. The mathematics are simplest if  $\theta_{14} = 0$  points directly away from the center. Again, use Figure (2.3) to see how this location is chosen. First, compare the value of the correlation function at the minimum attainable distance to the correlation functions at  $\theta_{14} = 0$  and  $\theta_{14} = \pi$ . If it is significantly larger (more than a factor of 3 or so), then calculate the location of intermediate values (approximately factors of the square root of 10) of the correlation function. Then choose  $\theta_{14}$  by the probabilities given by a power law fit to these values and locations. If the variation of the correlation is small, choose  $\theta_{14}$  uniformly. To calculate  $\phi_{14}$ , first determine which values of  $\phi_{14}$  lie in one of the slices. Then multiply the length within each slice by the value of the correlation function at the minimum separation available in that slice. This is possible because the minimum separation in the slice will be at one of the ends of the slice or at the minimum separation possible given  $\theta_{14}$ . Use this value to be the probability of choosing this slice. Once the slice is determined, compare the highest value of the correlation function within the slice to the lowest value. If the highest value is more than three times as high as the lowest, compute the positions along the slice of the predetermined values of the correlation function. (If it is not, again use a uniform distribution.) Once again, fit a power law to the determined values and locations and call this the probability distribution (this time for  $\phi_{14}$ ). Once the calculation of the position of galaxy four is complete, determine whether or not galaxy four is within the catalog.

If all of the galaxies are within the catalog, then compute the value of the integrand at that set of positions. In particular, take the product of the correlation functions of the separations ( $r_{14}$  and  $r_{23}$ ), the window functions, and the accumulated renormalizations due to the non-uniform probability functions for each variable. Then add this to the running total. Continue choosing

galaxy foursomes until the statistical error is below the error limit, at which point the value of the integral is the running total divided by the number of foursomes (including foursomes which were not in the catalog) times the 10-dimensional volume of the integral. This, of course, gives the value of the signal-signal portions of the matrix  $K$ . To find the full value of the matrix add into the matrix the components due to the delta functions (the 7-dimensional and 5-dimensional components). Then use this matrix in our calculation of the Fisher matrix.

### 2.3 Comparison of Fisher Matrices

By comparing the Fisher matrices calculated by two different methods, one can compare the relative accuracies of the two methods in measuring a particular set of parameters. In particular, in this section we compare the Fisher matrix as calculated by the pair weight method to an accepted method, the classical approximation, for the parameters  $P(k)$ . This will allow a comparison of the two methods to see whether or not the more complicated pair weight method is also the more accurate method. In particular, we would like to know which circumstances demand the pair weight method and which can be addressed by the more easily computed classical method. Note that in this comparison we are comparing the Fisher matrices of Gaussian models with no redshift distortions.

#### 2.3.1 Classical Method Versus Pair Weight Method for IRAS 1.2Jy

The IRAS 1.2 Jy redshift survey is nearly all-sky. This means that the classical approximation should work very well. This makes it a good choice for comparison between the pair weight method and the classical method. To generate the Fisher matrices, we need to make assumptions about the prior prediction of the power spectrum (or, equivalently, about the correlation function). Our power spectrum was generated by the methods described in Eisenstein and Hu (1999) with  $h = 0.65$ ,  $\Omega_\Lambda = 0.7$ ,  $\Omega_b = 0.3$ ,  $n = 1$ , and  $T = 2.73$  K. For this comparison, we use a Fisher matrix calculated as described in Hamilton (1997) for the classical method. For

the pair weight method, we use one window at each separation. The window is given by

$$W_{\alpha ij} = \frac{\bar{n}_i \bar{n}_j \delta(r_\alpha - |\mathbf{r}_i - \mathbf{r}_j|)}{(1 + 4\pi J_{3\alpha} \bar{n}_i)(1 + 4\pi J_{3\alpha} \bar{n}_j)} \quad (2.30)$$

where

$$J_{3\alpha} = \int_0^{r_\alpha} r^2 \xi(r) dr. \quad (2.31)$$

We expect this window to reflect the information content because we are counting equal volumes in regions where the distribution is well sampled and equal numbers where it is sparsely sampled.

To compare the information contained within the Fisher matrix, we would like to find statistically independent variables and find the amount of information about each of these variables contained within the data set. Hamilton and Tegmark (2000a) describes a number of ways to decorrelate the data. In this paper we will use the Fisher matrix divided by the prior value of the power spectrum at the particular  $k$  (the fractional Fisher matrix) rather than the Fisher matrix itself.

$$G_{\alpha\beta} \equiv \left[ \xi_\alpha^{-1} \langle \Delta \hat{\xi}_\alpha \Delta \hat{\xi}_\beta \rangle \xi_\beta^{-1} \right]^{-1} = \xi_\alpha F_{\alpha\beta} \xi_\beta. \quad (2.32)$$

This is so that the fractional error is the error in question rather than the absolute error. This means that the region where  $\xi$  is large will not be over-represented in regions where  $\xi$  is small. To decorrelate this matrix, measure the parameters which are the rows (normalized to unit sum) of the square-root of this matrix. This ensures that these parameters will be decorrelated with eigenvalue equal to the unnormalized sum of the row squared ( $[\sum_i F_{ij}^{1/2}]^2$ ). Compare two quantities between the two matrices. The first is addressed in Figure 2.4. This Figure shows a set of normalized rows of the square-root of the Fisher matrices. (Solid is the pair weight method and dashed is the classical method.) These are the actual parameters that we will measure. Notice two things about this Figure. First, the parameters have narrow peaks centered on the wavelength in question. This means that the decorrelated parameter does a good job of measuring the value of the power spectrum at a particular  $k$ . Second, notice that the peak of the

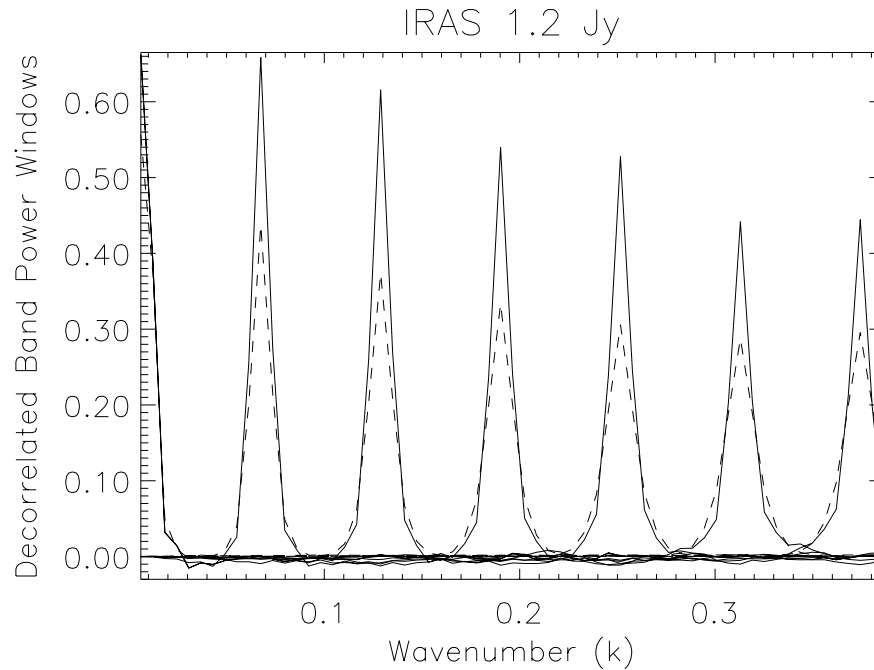


Figure 2.4: Normalized rows of the square-root of the Fisher matrix. Solid lines are for the pair weight method and dashed are for the classical method.

parameter is higher for the pair weight method than it is for the classical method. This is due to the fact that the pair weight method has values off the diagonal which are negative. These negative values are likely to be caused by errors in the calculation of the Fisher matrix rather than actual regions of negative information. Because the Fisher matrix is used in the calculation of the parameters from the data as well as to estimate the accuracy of the calculation, errors in the calculation of the Fisher matrix will reduce the accuracy with which the parameters in question can be measured.

Figure 2.5 depicts the amount of information contained within the IRAS catalog in the decorrelated band-powers. The classical method extracts as much (or more) information about the parameters on all scales as does the pair weight compression method with one window per separation. This is not too surprising due to the fact that the IRAS catalog is nearly all-sky. This means that the classical approximation should be very nearly valid. This also means that

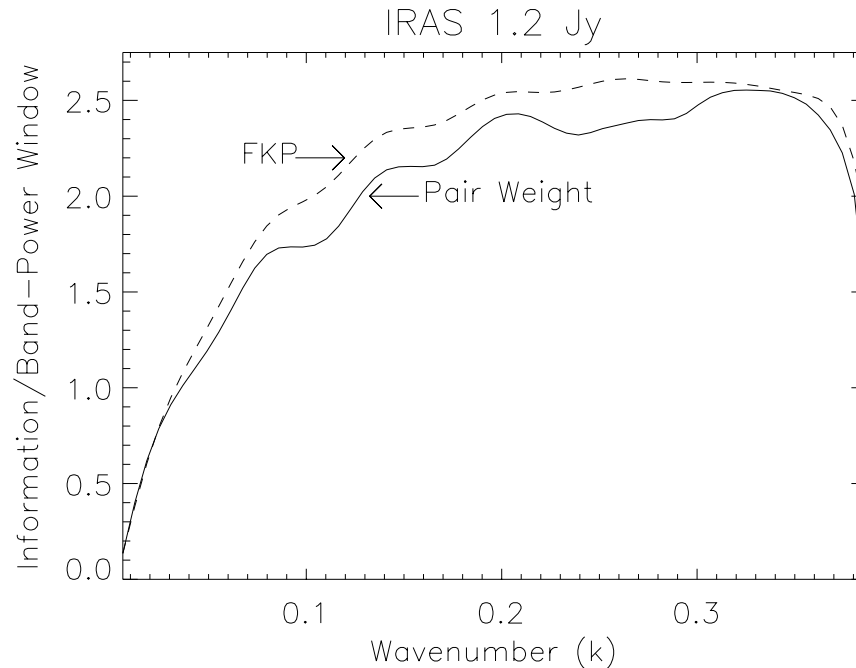


Figure 2.5: Information contained within decorrelated parameters. The  $k$  index gives the wavenumber of the location of the peak of the parameter. The solid line is for the pair weight method and the dashed line is for the classical method.

for a catalog such as IRAS, one should strongly consider using the simpler classical method on the small to moderate scales. On the largest scales, one should use one of the brute-force techniques. These techniques should eliminate the approximation used in the classical method while still being feasible.

### 2.3.2 Classical Method Versus Pair Weight Method for LCRS

The Las Campanas Redshift Survey (Shectman et al., 1996) allows us to compare the pair weight method to the classical method in a situation where we expect the classical approximation to break down. LCRS has 327 fields approximately  $1.5^\circ \times 1.5^\circ$  contained within 6 slices. In each of these fields up to 112 redshifts were taken. Due to the limitations of the observing procedure, each field has its own selection function. (The selection function depends upon the fraction of galaxies in the field that have redshifts. This fraction varies from field to field.) This

means that the largest length scale over which the catalog does not vary is  $1.5^\circ$  ( $\approx 7.5h^{-1}$  Mpc at the median depth of the survey). On scales larger than this the classical approximation should lose some of the available information. The complications of the LCRS catalog also make many of the brute force calculations difficult, though not impossible.

In addition to probing a region where the classical method should be inadequate, we wanted to investigate the benefits of using more than one window at each separation. Using more than one set of windows, should enable the extraction of more information than with only one set. We would like to know whether the additional information contained within the additional windows is enough to justify the computing cost. The windows we used for this are the same as those defined in equation 2.30 with four different choices of  $J_{3\alpha}$ . The four windows have

$$J'_{3\alpha} = 0, J_{3\alpha}/10, J_{3\alpha}, 10J_{3\alpha} \quad (2.33)$$

respectively. We chose these windows to make sure that the information contained within one window was sufficiently different from the next.

Once again, our power spectrum was generated by the methods described in Eisenstein and Hu (1999) with  $h = 0.65$ ,  $\Lambda = 0.7$ ,  $\Omega_b = 0.3$ ,  $n = 1$ , and  $T = 2.73$  K. For the classical approximation, we again use a Fisher matrix calculated as described in Hamilton (1997). The plots of the information contained within the Fisher matrices in this section have been calculated in the same way as those of the previous section. Because the differences between the pair weight method and the classical method should be largest on scales larger than  $\approx 7.5h^{-1}$  Mpc and because the difference between one window and four should be apparent on all scales, we have only calculated a  $31 \times 31$  matrix of separations.

In Figure 2.6 is the information contained within all four sets of windows (the solid line) and the information contained within each set of windows individually. It is clear that adding windows does, in fact, allow for the extraction more information. However, notice that the information contained within the best set of windows (this happens to be the third window,

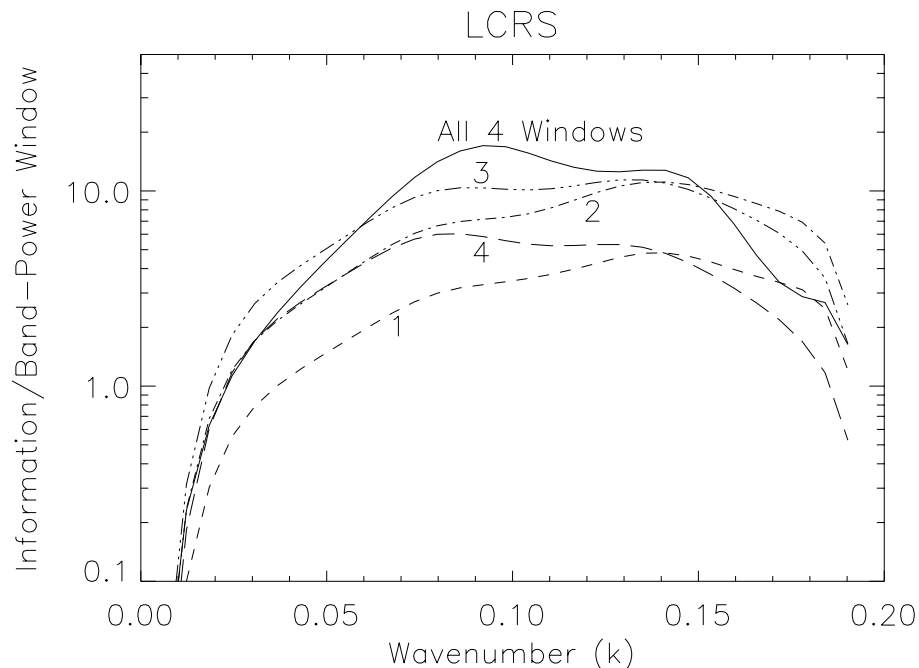


Figure 2.6: Information contained within decorrelated parameters for the pair weight method. The  $k$  index gives the wavenumber of the location of the peak of the parameter. The solid line contains information from all four sets of windows. The four other lines contain only the information from one of the sets of windows.

with  $\hat{J}_{3\alpha} = J_{3\alpha}$ ) contains no less than half of the information on all scales (as compared to the complete set of four windows). This Figure shows that this window actually contains more information on the smaller scales. This window does not actually contain more information but rather the errors in the method of calculation yield slightly inaccurate results. Also note that the fourth window ( $\hat{J}_{3\alpha} = 10J_{3\alpha}$ ) appears to contain the second most information of all the sets of windows. However, after eliminating this set of windows from the calculation, the remaining three sets of windows contain almost exactly the same amount of information as do all four sets together. The information extracted by window four has already been extracted by the first three windows (primarily window three).

Figure 2.7 shows the information contained within the classical approximation as compared to the pair weight method. This plot shows that on the very largest scales (small  $k$ ) the

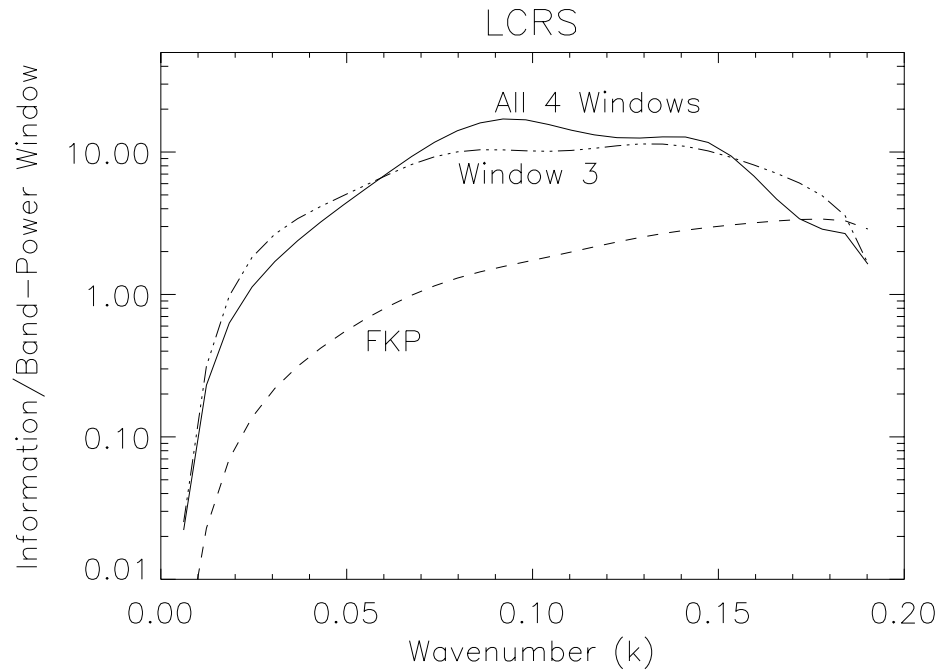


Figure 2.7: Information contained within decorrelated parameters. The  $k$  index gives the wavenumber of the location of the peak of the parameter. The solid line contains information from all four sets of windows for the pair weight method. The dot-dashed line is the information contained within the best single window for the pair weight method. The dashed line shows the information contained within the classical method.

pair weight method contains several times as much information as does the classical method. On smaller scales, the difference becomes less. On the smallest scales the classical method does retain more information than does this pair weight method. There are two causes for this. One cause is aliasing in the FFT used to go from real space to Fourier space. We found (in Chapter 4) that the latter portion of the matrices are contaminated to some degree by aliasing. Second, when the calculation is extended to include smaller scales, it does a better job of retaining the information on larger scales as well. This is particularly important for elements near the edge of the matrix. To obtain the best measurements of the power spectrum on these scales one would have to extend the Fisher matrix calculation to smaller scales.

The decorrelated band-powers, for which the information is calculated, are shown in Figure 2.8. Once again the parameters are narrow about the peak. Also, notice that the classical

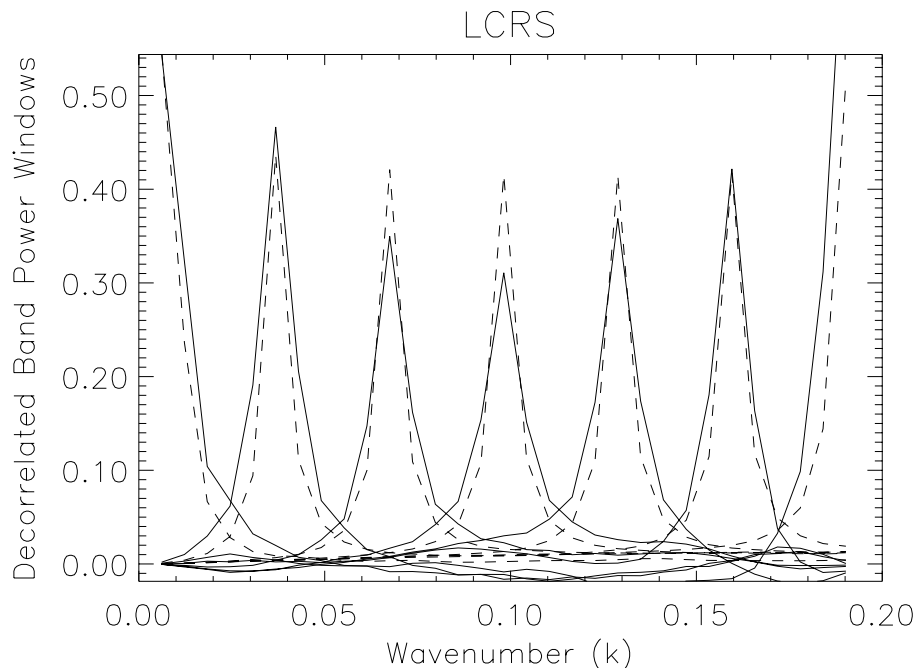


Figure 2.8: Normalized rows of the square-root of the Fisher matrix. Solid lines are for the pair weight method and dashed are for the classical method.

method parameters are very similar to the pair weight parameters. The main difference between the two is that the errors in the calculation of the pair weight Fisher matrix once again causes regions where the square root of the Fisher matrix is negative. This means that the errors in the calculation of the Fisher matrix is causing us to measure the parameters with weights which are not the best choice and to measure them with less accuracy than would be possible if the integrals of the matrix elements could be done exactly. Notice that, in the case for LCRS, the errors in the pair weight calculation mainly affect the smallest and largest scales measured while not greatly affecting the intermediate scales.

For the LCRS catalog, the pair weight method provides a more accurate measurement for the largest scales than does the classical method. Unfortunately, with only our  $31 \times 31$  matrix of data points we are unable to say for sure where the classical method becomes comparable to the pair weight method.

## 2.4 Discussion and Conclusions

We introduced a pair weight compression technique for measuring the power spectra from galaxy catalogs. This method requires the calculation of a matrix of ten-dimensional integrals. Because galaxy surveys tend to be less than all-sky, we found that the integrals cannot be performed analytically or by traditional numerical techniques. We discussed a Monte Carlo technique for computing these integrals. The advantage of the Monte Carlo technique is that the integrals can be performed even when the catalog's selection function is very complex (as is the case for LCRS). We then applied the technique to the IRAS 1.2 Jy redshift catalog and the LCRS.

We found that for the IRAS 1.2 Jy survey, the classical method would produce (slightly) smaller error bars than would the pair-weight method, if we use just one window per separation. Both methods are able to measure narrowly peaked decorrelated band-powers. Although the pair weight method works for a nearly all sky survey like IRAS, it is clear that the simplicity of the classical method makes it the preferred method of calculation.

For LCRS, we found that even using only one window per separation, the pair weight method produces error bars considerably smaller (as much as a factor of three smaller) than those of the classical method. When we used four (or the three best), windows per separation the information retained was even greater. Due to the computational expense of calculating the additional windows, it is not clear whether one should use one or more window per separation. Clearly, if computational expense is not an issue, one should use many windows.

Throughout the chapter we have assumed that the overdensities are linear and that redshift distortions are negligible. We know that both of these assumptions are not accurate in our universe. Under these simplified circumstances, we saw that the pair weight method is a viable method. For surveys with complicated selection functions, the pair weight method might well be the preferred method. It will be interesting to see whether the pair weight method remains a quality method when we relax the assumptions of linearity and small distortions.